Electron Paramagnetic Resonance and Spectroscopic Characteristics of Electrogenerated Mixed-Valent Systems [(η 5 -C 5 Me 5)M(μ-L)M(η 5 -C 5 Me 5)] + (M = Rh, Ir; L = 2,5-Diiminop...

ARTICLE *in* INORGANIC CHEMISTRY · JULY 2000

Impact Factor: 4.76 · DOI: 10.1021/ic991110d · Source: PubMed

5 AUTHORS, INCLUDING:

Axel Klein
University of Cologne
185 PUBLICATIONS **2,897** CITATIONS

SEE PROFILE

Electron Paramagnetic Resonance and Spectroscopic Characteristics of Electrogenerated Mixed-Valent Systems $[(\eta^5\text{-}C_5Me_5)M(\mu\text{-}L)M(\eta^5\text{-}C_5Me_5)]^+$ (M = Rh, Ir; L = 2,5-Diiminopyrazines) in Relation to the Radicals $[(\eta^5\text{-}C_5Me_5)ClM(\mu\text{-}L)MCl(\eta^5\text{-}C_5Me_5)]^+$ and $[(\eta^5\text{-}C_5Me_5)M(\mu\text{-}L)MCl(\eta^5\text{-}C_5Me_5)]^{2+}$

Sascha Berger, Axel Klein, Matthias Wanner, and Wolfgang Kaim*

Institut für Anorganische Chemie der Universität, Pfaffenwaldring 55, D-70550 Stuttgart, Germany

Jan Fiedler

J. Heyrovsky Institute of Physical Chemistry, Academy of Sciences of the Czech Republic, Dolejškova 3, CZ-18223 Prague, Czech Republic

Received September 16, 1999

Electrochemical reduction of the dinuclear $[(\eta^5\text{-}C_5Me_5)ClM(\mu\text{-}L)MCl(\eta^5\text{-}C_5Me_5)]^{2+}$ ions (M = Rh, Ir; L = 2,5-bis(1-phenyliminoethyl)pyrazine (bpip) and 2,5-bis[1-(2,6-dimethylphenyl)iminoethyl]pyrazine (bxip)) proceeds via the paramagnetic intermediates $[(\eta^5\text{-}C_5Me_5)ClM(\mu\text{-}L)MCl(\eta^5\text{-}C_5Me_5)]^+$ (L = bpip) or $[(\eta^5\text{-}C_5Me_5)M(\mu\text{-}L)\text{-}MCl(\eta^5\text{-}C_5Me_5)]^{2+}$ (L = bxip) and $[(\eta^5\text{-}C_5Me_5)M(\mu\text{-}L)M(\eta^5\text{-}C_5Me_5)]^+$. Whereas the first is clearly a radical species with a small *g* anisotropy, the chloride-free cations are distinguished by structured intervalence charge transfer (IVCT) bands in the near-infrared region and by rhombic electron paramagnetic resonance features between $g = 1.9$ and $g = 2.3$, which suggests considerable metal participation at the singly occupied MO. Alternatives for the d configuration assignment and for the role of the bisbidentate-conjugated bridging ligands will be discussed. The main difference between bpip and bxip systems is the destabilization of the chloride-containing forms through the bxip ligand for reasons of steric interference.

Introduction

In contrast to the numerous mixed-valent complexes $L_nM^k\text{-}(\mu\text{-}L)M^{k+1}L_n$ with d^5/d^6 configurated metal centers M and bridging ligands L,[1−6] there have been relatively few[7−13] such compounds with other d^{n-1}/d^n configurations. In the course of research on the coupling of organometallic redox reaction centers through mediating bridging ligands $\mu;\eta^4$-L,[14−18] we have now been able to study the systems $[(\eta^5\text{-}C_5Me_5)M(\mu\text{-}L)M(\eta^5\text{-}C_5Me_5)]^+$ (M = Rh, Ir; L = 2,5-bis(1-phenyliminoethyl)pyrazine (bpip) or 2,5-bis[1-(2,6-dimethylphenyl)iminoethyl]pyrazine (bxip) by electron paramagnetic resonance (EPR) and by

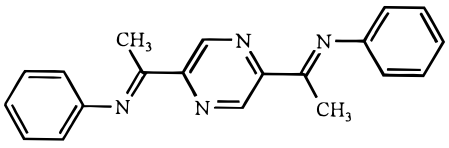

bpip

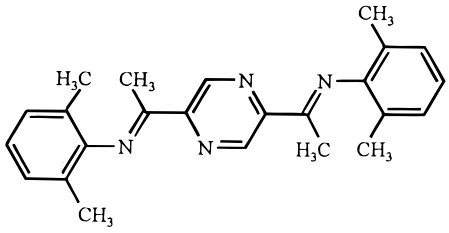

bxip

absorption spectroscopy in the near-infrared, the typical region for intervalence charge transfer (IVCT) transitions. These results, as obtained through in situ EPR and OTTLE (optically transpar-

(1) Creutz, C. *Progr. Inorg. Chem.* **1983**, *30*, 1.
(2) Richardson, D. E.; Taube, H. *Coord. Chem. Rev.* **1984**, *60*, 107.
(3) Crutchley, R. J. *Adv. Inorg. Chem.* **1994**, *41*, 273.
(4) Ward, M. D. *Chem. Soc. Rev.* **1995**, *34*, 121.
(5) Bruns, W.; Kaim, W.; Waldhör, E.; Krejcik, M. *J. Chem. Soc., Chem. Commun.* **1993**, 1868.
(6) Bruns, W.; Kaim, W.; Waldhör, E.; Krejcik, M. *Inorg. Chem.* **1995**, *34*, 663.
(7) Robin, M. B.; Day, P. *Adv. Inorg. Chem. Radiochem.* **1967**, *10*, 247.
(8) Prassides, K., Ed. In *Mixed Valency Systems—Applications in Chemistry, Physics and Biology*; Kluwer Academic Publishers: Dordrecht, 1991.
(9) LeCloux, D. D.; Davydov, R.; Lippard, S. J. *Inorg. Chem.* **1998**, *37*, 6814.
(10) Ball, J. M.; Boorman, P. M.; Fait, J. F.; Kraatz, H. B.; Heinz, B.; Richardson, J. F.; Collison, D.; Mabbs, F. E. *Inorg. Chem.* **1990**, *29*, 3290.
(11) Schake, A. R.; Schmitt, E. A.; Conti, A. J.; Streib, W. E.; Huffman, J. C.; Hendrickson, D. N.; Christou, G. *Inorg. Chem.* **1991**, *30*, 3192.
(12) Limburg, J.; Vrettos, J. S.; Liable-Sands, L. M.; Rheingold, A. L.; Crabtree, R. H.; Brudvig, G. W. *Science* **1999**, *283*, 1524.
(13) Brooker, S.; Kelly, R. J.; Plieger, P. G. *J. Chem. Soc., Chem. Commun.* **1998**, 1079.
(14) Kasack, V.; Kaim, W.; Binder, H.; Jordanov, J.; Roth, E. *Inorg. Chem.* **1995**, *34*, 1924.
(15) Ketterle, M.; Fiedler, J.; Kaim, W. *J. Chem. Soc., Chem. Commun.* **1998**, 1701.
(16) Stahl, T.; Kasack, V.; Kaim, W. *J. Chem. Soc., Perkin Trans. 2* **1995**, 2127.
(17) Klein, A.; Kasack, V.; Reinhardt, R.; Sixt, T.; Scheiring, T.; Zalis, S.; Fiedler, J.; Kaim, W. *J. Chem. Soc., Dalton Trans.* **1999**, 575.
(18) Klein, A.; Hasenzahl, S.; Kaim, W.; Fiedler, J. *Organometallics* **1998**, *17*, 3532.

10.1021/ic991110d CCC: $19.00
Published on Web 05/20/2000

ent thin-layer electrolysis)[19] spectroelectrochemistry, will be compared with the EPR and UV/vis/NIR data of related paramagnetic precursor complexes $[(\eta^5\text{-}C_5Me_5)ClM(\mu\text{-}L)MCl(\eta^5\text{-}C_5Me_5)]^+$ and $[(\eta^5\text{-}C_5Me_5)M(\mu\text{-}L)MCl(\eta^5\text{-}C_5Me_5)]^{2+}$.

Bpip has been used in a number of cases[16−18,20,21] as a symmetrically bisbidentate-conjugated bridging ligand containing a central pyrazine ring that, in unsubstituted form, is the bridge in the prototypical mixed-valent Creutz−Taube ion.[1−4,22,23] The bxip ligand is presented here for the first time. Its conception was based on structural results obtained for a pentamethylcyclopentadienyliridium complex of 1,4-bis(2,6-dimethylphenyl)-1,4-diazabutadiene,

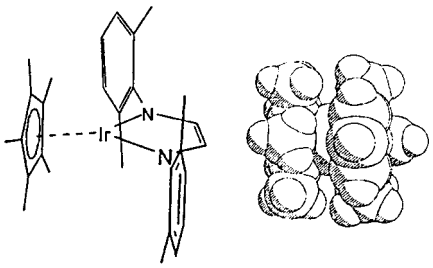

which revealed electronic as well as steric stabilization of the coordinatively unsaturated metal center.[24−26]

Experimental Section

Materials. The ligand bpip and the complexes $[(\eta^5\text{-}C_5Me_5)ClM(\mu\text{-bpip})MCl(\eta^5\text{-}C_5Me_5)](PF_6)_2$ have been described previously.[16−18,20,21]

The ligand bxip was prepared as follows. A mixture containing 2,5-diacetylpyrazine (100 mg, 0.609 mmol), freshly distilled 2,6-dimethylaniline (238 mg, 1.34 mmol), 4 Å molecular sieves (3 g), and acidic alumina (20 mg) was heated in toluene (50 mL) under reflux for 24 h. The hot solution was filtered and reduced in volume to 30 mL, and the yellow crystals were collected. Washing with *n*-heptane, recrystallizing from diethyl ether, and drying under vacuum yielded the pale-yellow product in 109 mg yield (48%). Found: C, 76.54; H, 8.26; N, 14.06%. $C_{24}H_{30}N_4$ (374.53) requires C, 76.97; H, 8.07; N, 14.96%. NMR δ_H (acetone-d_6): 2.12 (12H, s, CH_3), 2.68 (6H, s, CH_3), 6.45 (2H, t, CH_{Ph}), 6.82 (4H, d, CH_{Ph}), 9.17 (2H, s, CH_{pz}) ppm; ^3J (CH_{Ph}) = 7.45 Hz.

The complexes $[(\eta^5\text{-}C_5Me_5)ClM(\mu\text{-bxip})MCl(\eta^5\text{-}C_5Me_5)](PF_6)_2$ were obtained in a similar manner as the bpip compounds[20,21] by reacting $[M(\eta^5\text{-}C_5Me_5)Cl_2]_2$ with 2 equiv of $AgPF_6$ in acetone, filtration, and addition of the free bridging ligand (1 equiv). After 1 h the deeply colored solutions were filtered and reduced in volume, and the filtrate was then treated with 1 equiv of Bu_4NPF_6 to yield the purplish-black (Ir) or brown-red (Rh) product in about 70% yield.

$[(\eta^5\text{-}C_5Me_5)ClIr(\mu\text{-bxip})IrCl(\eta^5\text{-}C_5Me_5)](PF_6)_2$ (cis (A) and trans (B) isomers in 1:3 ratio). Found: C, 37.62; H, 4.21; N, 3.60%. $C_{44}H_{56}Cl_2F_{12}Ir_2N_4P_2$ (1390.27) requires C, 38.12; H, 4.07; N, 4.04%. NMR δ_H (CD_3NO_2): 1.65 (A) and 1.66 (B) (s, 30H, ($\eta^5\text{-}C_5Me_5$)), 2.29 (B) and 2.35 (A) (s, 6H, CH_3(phenyl)), 2.44 (B) and 2.45 (A) (s, 6H, CH_3(phenyl)), 2.82 (B) and 2.87 (A) (s, 6H, CH_3(imine)), 7.48 (A,B) (m, 6H, CH_{Ph}), 9.57 (B) and 9.58 (A) (s, 2H, CH_{pz}) ppm.

$[(\eta^5\text{-}C_5Me_5)ClRh(\mu\text{-bxip})RhCl(\eta^5\text{-}C_5Me_5)](PF_6)_2$ (cis and trans isomers in 1:1 ratio). Found: C, 43.84; H, 5.28; N, 4.88%. $C_{44}H_{56}Cl_2F_{12}N_4P_2Rh_2$ (1207.62) requires C, 43.67; H, 4.67; N, 4.64%. NMR δ_H (CD_3NO_2): 1.64 and 1.65 (s, 30H, ($\eta^5\text{-}C_5Me_5$)), 2.22 and 2.25 (s, 6H, CH_3(phenyl)), 2.46 and 2.48 (s, 6H, CH_3(phenyl)), 2.83 and 2.86 (s, 6H, CH_3(imine)), 7.50 (m, 6H, CH_{Ph}), 9.57 and 9.58 (s, 2H, CH_{pz}) ppm.

Instrumentation. EPR spectra were recorded in the X band on a Bruker System ESP 300 equipped with a Bruker ER035M gauss meter and a HP 5350B microwave counter. A continuous flow cryostat ESR 900 from Oxford Instruments was used for liquid He cooling. ^{1}H NMR spectra were taken on a Bruker AC 250 spectrometer, and UV/vis/NIR absorption spectra were recorded on a Bruins Instruments Omega 10 spectrophotometer. Cyclic voltammetry was carried out in solutions containing 0.1 mol dm^{-3} in Bu_4NPF_6 using a three-electrode configuration (glassy carbon working electrode, Pt counter electrode, Ag/AgCl reference) and a PAR 273 potentiostat and function generator. The ferrocene/ferrocenium couple served as an internal reference. Digital simulation was performed using the program ESP (C. Nervi)[26] suitable for staircase voltammetry. Spectroelectrochemical measurements were performed using an optically transparent thin-layer electrode (OTTLE, Pt-grid) cell[19] for UV/vis spectra and a two-electrode capillary for EPR studies.[27]

Results and Discussion

Characterization of Precursors. The precursor complexes $[(\eta^5\text{-}C_5Me_5)ClM(\mu\text{-bpip})MCl(\eta^5\text{-}C_5Me_5)](PF_6)_2$, M = Rh and Ir, have been described previously.[20,21] The new compounds bxip and $[(\eta^5\text{-}C_5Me_5)ClM(\mu\text{-bxip})MCl(\eta^5\text{-}C_5Me_5)](PF_6)_2$ were prepared accordingly. The complexes were obtained as mixtures of cis and trans isomers

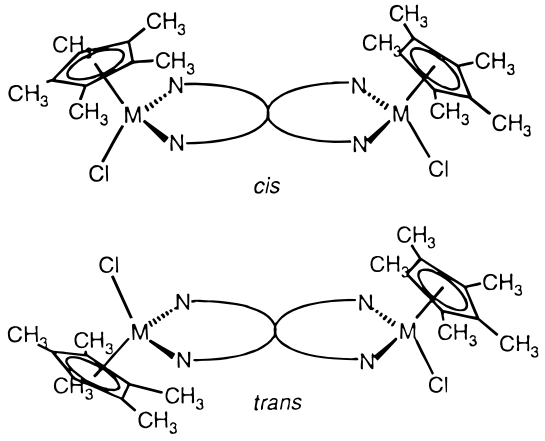

with respect to the arrangement of Cl and ($\eta^5\text{-}C_5Me_5$) ligands vs the central molecular plane, which, however, does not significantly affect the EPR and (spectro)electrochemical results.[20,21,28]

Cyclic Voltammetry. Dinuclear complex ions of the general formula $[(C_nR_n)HalM(\mu\text{-L})MHal(C_nR_n)]^{2+}$, n = 5 and M = Rh or Ir, n = 6 and M = Ru and Os, are known to undergo typical electron transfer/atom transfer sequences as depicted in the Scheme 1.[20,21,28] Essential features of this scheme as elucidated by cyclic voltammetry are the reversible one-electron reduction (at potential E_1) of the precursor dications before a second electron (at E_2) causes the first chloride dissociation ("electron reservoir" behavior of L)[20,21,28] and the dissociative third one-electron addition at E_3, which leads to a chloride-free mixed-valent intermediate. The fourth electron at E_4 produces a neutral

(19) Krejcik, M.; Danek, M.; Hartl, F. *J. Electroanal. Chem. Interfacial Electrochem.* **1991**, *317*, 179.
(20) Kaim, W.; Reinhardt, R.; Fiedler, J. *Angew. Chem.* **1997**, *109*, 2600. Kaim, W.; Reinhardt, R.; Fiedler, J. *Angew. Chem., Int. Ed. Engl.* **1997**, *36*, 2493.
(21) Kaim, W.; Berger, S.; Greulich, S.; Reinhardt, R.; Fiedler, J. *J. Organomet. Chem.* **1999**, *582*, 153.
(22) Creutz, C.; Taube, H. *J. Am. Chem. Soc.* **1969**, *91*, 3988; **1973**, *95*, 1086.
(23) Creutz, C.; Chou, M. H. *Inorg. Chem.* **1987**, *26*, 2995.
(24) Greulich, S.; Kaim, W.; Stange, A.; Stoll, H.; Fiedler, J.; Zalis, S. *Inorg. Chem.* **1996**, *35*, 3998.
(25) Reinhardt, R.; Kaim, W. *Z. Anorg. Allg. Chem.* **1993**, *619*, 1998.
(26) Program ESP (Nervi, C.), available at http//lem.ch.unito.it/chemistry/esp_manual.html.
(27) Kaim, W.; Ernst, S.; Kasack, V. *J. Am. Chem. Soc.* **1990**, *112*, 173.
(28) Baumann, F.; Stange, A.; Kaim, W. *Inorg. Chem. Commun.* **1998**, *1*, 305.

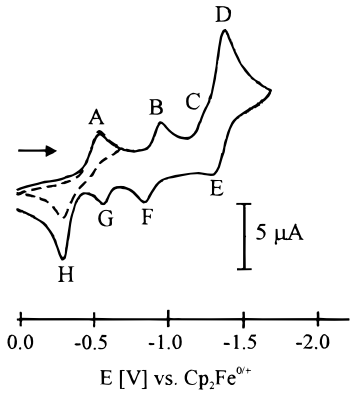

Figure 1. Cyclic voltammograms of $[(\eta^5\text{-}C_5Me_5)ClRh(\mu\text{-bxip})RhCl(\eta^5\text{-}C_5Me_5)](PF_6)_2$ in DMF/0.1 M Bu_4NPF_6 at 100 mV/s.

compound that may be reduced one more time at very negative potentials (E_5).

The main difference between corresponding bpip and bxip compounds as now observed here lies in the diminished reversibility of the first ligand-centered reduction for the bxip complexes (Figure 1). While the expected cathodic shift of potentials due to the introduction of electron-releasing methyl substituents is marginal, the apparent and structurally documented[24] steric effect of the space-filling 2,6-dimethylphenyl group is to disfavor the more congested chloride-containing M(III) precursor and to kinetically stabilize the chloride-free system with its lower coordination number at the metal center. Accordingly, the diiridium complex of the bxip ligand exhibits a cyclic voltammetric response with two return peaks (E_1^{pa}, E_{1x}^{pa}) for the first reduction process, corresponding to chloride-containing and chloride-free species (Table 1).[25] For the rhodium system, the reversible counterpeak relating to chloride-containing species is detectable at $E^{pa} = -0.46$ V only at scan rates above 500 mV/s. In contrast to the situation for bpip complexes,[21] the reoxidation peaks are well separated in the case of the bxip analogues, which allows for an evaluation of the rate constants for chloride dissociation from $[(\eta^5\text{-}C_5Me_5)ClM(\mu\text{-bxip})MCl(\eta^5\text{-}C_5Me_5)]^+$. The values $k = 5.9 \pm 0.9\ s^{-1}$ and $k = 1.1 \pm 0.2\ s^{-1}$ for M = Rh and M = Ir, respectively,

Table 1. Peak Potentials from Cyclic Voltammetry[a] of Complexes $[(\eta^5\text{-}C_5Me_5)ClM(\mu\text{-L})MCl(\eta^5\text{-}C_5Me_5)](PF_6)_2$

	μ-L = bpip		μ-L = bxip	
E[b]	M = Ir	M = Rh	M = Ir	M = Rh
E_1^{pc}	−0.44	−0.50	−0.46	−0.53
E_2^{pc}	−0.83	−0.76	−0.78	−0.93
E_3^{pc}	−1.54[c]	−1.25	−1.52[c]	−1.23
E_4^{pc}	−1.54[c]	−1.39	−1.52[c]	−1.37
E_5^{pc}	<−2.7	−2.45	−2.69	−2.27
E_{1x}^{pa}			−0.19[c]	−0.31[c]
E_{2x}^{pa}	−0.36[c]	−0.43[c]	−0.19[c]	−0.31[c]
E_1^{pa}	−0.36[c]	−0.43[c]	−0.39	
E_{2y}^{pa}			−0.52	−0.56
E_{3x}^{pa}	−1.23	−1.03	−1.10	−0.84
E_4^{pa}	−1.44	−1.33	−1.45	−1.31
E_5^{pa}	<−2.6	−2.37		−2.20

[a] In CH_3CN (bpip compounds) or DMF (bxip complexes) with 0.1 M Bu_4NPF_6 at 100 mV/s scan rate. Potentials vs $FeCp_2^{+/0}$. Superscript pc: cathodic peak. Superscript pa: anodic peak. [b] For identification of processes see scheme in the main text. [c] Two overlapping one-electron peaks according to spectroelectrochemistry.

were obtained by fitting the experimental cyclic voltammograms using the ESP[26] simulation program. (The fitting procedure was applied to experimental cyclic voltammograms involving the first two reduction and corresponding return peaks. The error limit refers to the standard deviation obtained from a set of cyclic voltammograms at different scan rates.)

The second reduction of $[(\eta^5\text{-}C_5Me_5)ClM(\mu\text{-bxip})MCl(\eta^5\text{-}C_5Me_5)]^{2+}$ (peak B in Figure 1) is followed by fast chloride dissociation; cyclic voltammetry within peak B does not exhibit any counterpeak at scan rates up to 10 V/s. Furthermore, no new anodic peak appears when the potential sweep is extended from the first reduction peak (A) behind the second (B); however, the cyclic voltammogram is then showing increased height of the reoxidation peak (H). Hence, the potentials of the reoxidation processes $[(\eta^5\text{-}C_5Me_5)M(\mu\text{-bxip})MCl(\eta^5\text{-}C_5Me_5)]^{+\rightarrow 2+\rightarrow 3+}$ are close, which results in the disproportionation of the species $[(\eta^5\text{-}C_5Me_5)M(\mu\text{-bxip})MCl(\eta^5\text{-}C_5Me_5)]^{2+}$. The electrode mechanism of the two-electron reduction of $[(\eta^5\text{-}C_5Me_5)ClM(\mu\text{-bxip})MCl(\eta^5\text{-}C_5Me_5)]^{2+}$ can thus be interpreted as consecutive one-electron transfers, coupled to a series of

Scheme 1

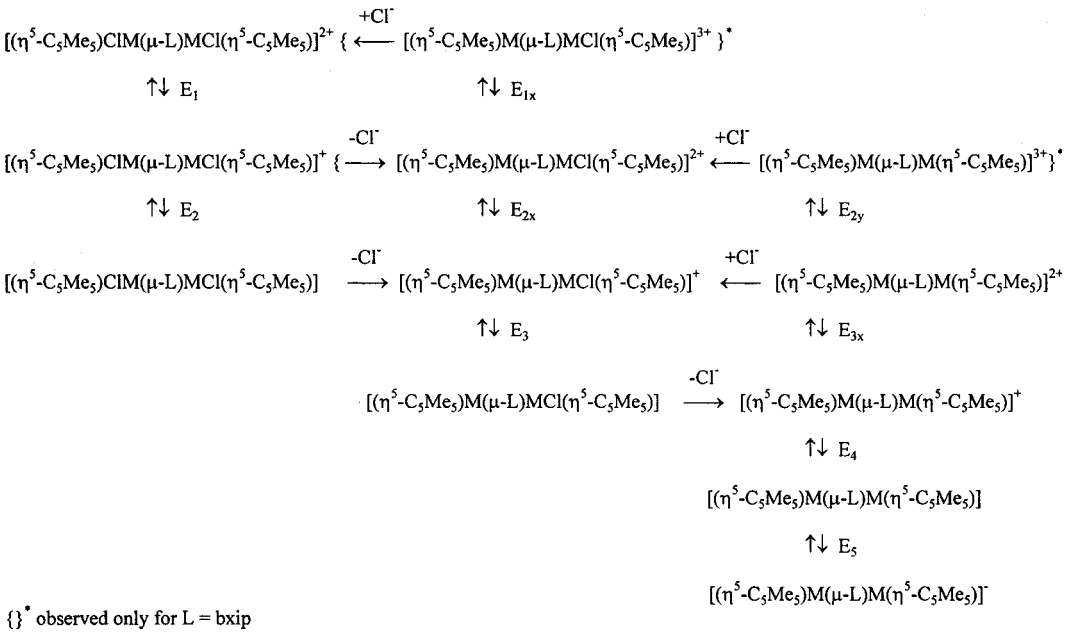

chemical reactions that include chloride dissociations, and a disproportionation equilibrium of the species $[(\eta^5\text{-}C_5Me_5)M(\mu\text{-bxip})MCl(\eta^5\text{-}C_5Me_5)]^{2+} \rightarrow [(\eta^5\text{-}C_5Me_5)M(\mu\text{-bxip})MCl(\eta^5\text{-}C_5Me_5)]^{+} + [(\eta^5\text{-}C_5Me_5)M(\mu\text{-bxip})MCl(\eta^5\text{-}C_5Me_5)]^{3+}$). Further evidence for the disproportionation reaction comes from the decreased height of the second reduction peak (B, when compared with A), clearly seen at low scan-rates, and from spectroelectrochemically observed direct formation of the two-electron reduction product during the first step of the electrolysis.

The mixed-valent species $[(\eta^5\text{-}C_5Me_5)M(\mu\text{-bxip})MCl(\eta^5\text{-}C_5Me_5)]^{+}$ undergoes the expected ECE reduction mechanism (overlapping peaks C, D), leading to the chloride-free species $[(\eta^5\text{-}C_5Me_5)M(\mu\text{-bxip})M(\eta^5\text{-}C_5Me_5)]$ via $[(\eta^5\text{-}C_5Me_5)M(\mu\text{-bxip})M(\eta^5\text{-}C_5Me_5)]^{+}$. Reoxidation at peaks E, F, G, H is a chemically reversible process during which chloride ions return to the coordination sphere (Scheme 1).

The singly reduced paramagnetic species $[(\eta^5\text{-}C_5Me_5)M(\mu\text{-bxip})MCl(\eta^5\text{-}C_5Me_5)]^{2+}$ could be electrogenerated in sufficient amounts for EPR spectroscopy. Similarly, the intermediate species $[Cp^*M(\mu\text{-L})MCp^*]^{+}$ could be characterized by EPR and OTTLE spectroelectrochemistry, although the difference between E_3^{pc} and E_4^{pc} can be quite small, ranging from 140 mV (M = Rh) to less than 50 mV (M = Ir). The pertinent values for the systems described in this work are summarized in Table 1.

The effect of metal replacement (Rh by Ir) results especially in cathodic shifts of E_3^{pc} and E_4^{pc}, confirming the interpretation of these processes as more metal-centered, in contrast to the presumably more ligand-centered processes E_1.

EPR Spectroscopy of Paramagnetic Intermediates. According to the redox scheme, at least two paramagnetic intermediates should be accessible in each case by prolonged electrolysis for in situ EPR characterization. Whereas the first, the one-electron reduction products of the precursor compounds, presented no problems and yielded relatively narrow signals at ambient temperatures, the next odd-electron species, the three-electron reduction products $[(\eta^5\text{-}C_5Me_5)M(\mu\text{-L})M(\eta^5\text{-}C_5Me_5)]^{+}$, were only observable by EPR at lower temperatures in glassy frozen solutions, indicating rapid relaxation and thus sizable 4d and 5d metal contributions. This contrast between the one- and three-electron reduction products is also confirmed immediately by the larger g anisotropy, Δg, of the latter, the spectra being distinguished by three well-separated g components (Figure 2, Table 2). The EPR spectra shown here also illustrate that—depending on the electrolysis conditions—both paramagnetic products can be detected simultaneously, owing to the EPR electrolysis cell design,[27] which allows for only slow vertical diffusion in a narrow tube.

Unfortunately, hyperfine coupling from metals (^{103}Rh ($I = {}^1/_2$, 100% natural abundance) or ^{191,193}Ir ($I = {}^3/_2$, 37.3 and 62.7% natural abundance))[29] or other nuclei such as ^{14}N could not be detected except for the previously described[20,21] $[(\eta^5\text{-}C_5Me_5)ClRh(\mu\text{-bpip})RhCl(\eta^5\text{-}C_5Me_5)]^{+}$ system. The other paramagnetic species exhibit broader lines due to unresolved hyperfine structure and higher g anisotropy (Table 2).

Although the chloride-containing radicals invariably exhibit Δg values smaller than those of the chloride-free species $[(\eta^5\text{-}C_5Me_5)M(\mu\text{-L})M(\eta^5\text{-}C_5Me_5)]^{+}$, the ratio between pertinent Δg values is much larger for the dirhodium systems (about 20) than for corresponding diiridium compounds (ca. 3.5). Alternatively, the difference between corresponding Rh and Ir species is very pronounced for the radicals $[(\eta^5\text{-}C_5Me_5)ClM(\mu\text{-L})MCl(\eta^5\text{-}C_5Me_5)]^{+}$ and $[(\eta^5\text{-}C_5Me_5)M(\mu\text{-L})MCl(\eta^5\text{-}C_5Me_5)]^{2+}$ but less marked for complexes $[(\eta^5\text{-}C_5Me_5)M(\mu\text{-L})M(\eta^5\text{-}C_5Me_5)]^{+}$. This result is somewhat unexpected, given the distinctly higher spin−orbit coupling factors of iridium (5d) relative to corresponding rhodium (4d) states.[29] For instance, the organometallic d^5/d^6 mixed-valent ions $[(R_3P)_2(OC)_3M(\mu\text{-L})M(CO)_3(PR_3)_2]^{+}$, L = pyrazine, R = isopropyl, and M = Mo, W, showed a much more pronounced difference between the 4d system (M = Mo: $g_\perp = 2.0655$, $g_\parallel = 1.9755$) and the 5d analogue (M = W: $g_1 = 2.197$, $g_2 = 2.158$, $g_3 = 1.931$).[5,6] However, a comparable EPR behavior as described here has been reported for $M^{I}M^{II}$ species with direct metal−metal interaction.[30]

Apart from the metal-dependent g anisotropy, Δg, there are few EPR differences between bpip and bxip containing compounds $[(\eta^5\text{-}C_5Me_5)M(\mu\text{-L})M(\eta^5\text{-}C_5Me_5)]^{+}$, and remarkably, the calculated average $\langle g\rangle$ is essentially identical at about $g = 2.055$ for all four systems (Table 2). In contrast, the chloride-containing radicals exhibit a much greater variety in terms of g splitting symmetry (axial or rhombic), Δg (strongly increased for Ir systems, larger for bxip than for bpip species), and $\langle g\rangle$

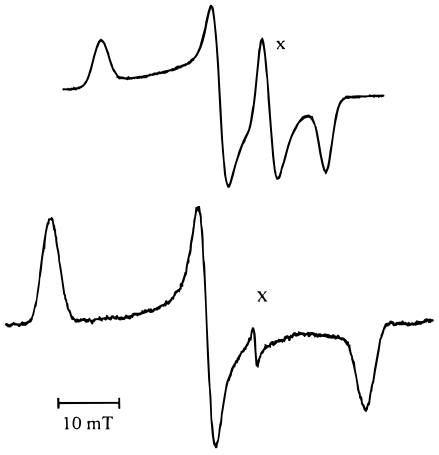

Figure 2. X band EPR spectra of $[(\eta^5\text{-}C_5Me_5)Rh(\mu\text{-bpip})Rh(\eta^5\text{-}C_5Me_5)]^{+}$ (upper spectrum) and $[(\eta^5\text{-}C_5Me_5)Ir(\mu\text{-bpip})Ir(\eta^5\text{-}C_5Me_5)]^{+}$ (lower spectrum), generated from cathodic three-electron reduction of precursors $[(\eta^5\text{-}C_5Me_5)ClM(\mu\text{-bpip})MCl(\eta^5\text{-}C_5Me_5)](PF_6)_2$ in DMF/0.1 M Bu_4NPF_6. The signals marked "x" are due to the respective $[(\eta^5\text{-}C_5Me_5)ClM(\mu\text{-bpip})MCl(\eta^5\text{-}C_5Me_5)]^{+}$ intermediates.

Table 2. g Factors of Paramagnetic Dirhodium and Diiridium Species[a]

M	L	g_1	g_2	g_3	Δg	$\langle g\rangle$
		$[(\eta^5\text{-}C_5Me_5)ClM(\mu\text{-L})MCl(\eta^5\text{-}C_5Me_5)]^{+}$				
Rh	bpip	1.9975	1.9975	1.990	0.0076	1.995[b]
Ir	bpip	2.009	2.000	1.916	0.093	1.975
		$[(\eta^5\text{-}C_5Me_5)M(\mu\text{-L})MCl(\eta^5\text{-}C_5Me_5)]^{2+}$				
Rh	bxip	2.015	2.001	1.996	0.019	2.004
Ir	bxip	2.0411	2.0068	1.9362	0.1049	1.995
		$[(\eta^5\text{-}C_5Me_5)M(\mu\text{-L})M(\eta^5\text{-}C_5Me_5)]^{+}$				
Rh	bpip	2.1656	2.0474	1.9516	0.2140	2.055
Rh	bxip	2.167	2.043	1.950	0.217	2.053
Ir	bpip	2.225	2.055	1.905	0.320	2.061
Ir	bxip	2.227	2.048	1.910	0.317	2.061

[a] Electrogenerated through cathodic reduction of precursors (Scheme 1) in CH_3CN/0.1 M Bu_4NPF_6 (bpip complexes) or DMF/0.1 M Bu_4NPF_6 (bxip systems). g values from simulations of spectra were taken at 3.5 K. [b] Hyperfine resolution (see ref 21).

(29) Weil, J. A.; Bolton, J. R.; Wertz, J. E. *Electron Paramagnetic Resonance*; Wiley: New York, 1994; p 533−536.

(30) (a) DeGray, J. A.; Rieger, P. H.; Connelly, N. G.; Garcia Herbosa, G. *J. Magn. Reson.* **1990**, *88*, 376. (b) Boyd, D. C.; Connelly, N. G.; Garcia Herbosa, G.; Hill, M. G.; Namm, K. R.; Mealli, C.; Orpen, A. G.; Richardson, K. E.; Rieger, P. H. *Inorg. Chem.* **1994**, *33*, 960.

(lower for Ir and bpip species). The main reason for this variability lies in the different composition, that is, $[(\eta^5\text{-}C_5Me_5)ClM(\mu\text{-bpip})MCl(\eta^5\text{-}C_5Me_5)]^+$ vs $[(\eta^5\text{-}C_5Me_5)M(\mu\text{-bxip})MCl(\eta^5\text{-}C_5Me_5)]^{2+}$. Apparently, the dissociation of one chloride already causes increased metal participation at the singly occupied MO (SOMO), indicated by larger Δg and $\langle g \rangle$ values. Part of the variability may also lie in structural differences between bpip and bxip complexes, the (partially) chloride-containing species with approximately tetrahedral configuration at the metal probably show a more sensitive response in terms of distortion toward the steric requirements resulting from the 2,6-dimethylphenyl substituent in bxip. As for Δg, the spin−orbit coupling constants of M(III) ions are higher than those of the corresponding metals in lower oxidation states, which could explain the strong increase of Δg on going from Rh(III) to Ir(III) radicals.

Isotropic or axial g component splitting is common for π radicals and their complexes, whereas rather symmetrical rhombic splitting has been observed for metal/ligand mixed situations at lower symmetries.[14] The higher $\langle g \rangle$ values for $[(\eta^5\text{-}C_5Me_5)M(\mu\text{-L})M(\eta^5\text{-}C_5Me_5)]^+$ relative to those of $[(\eta^5\text{-}C_5Me_5)ClM(\mu\text{-L})MCl(\eta^5\text{-}C_5Me_5)]^+$ reflect a situation known for most d^5/d^6 mixed-valent species, that is, occupied MOs lying rather close to the SOMO, which also causes low-energy IVCT transitions (HOMO → SOMO; see below).[5,6] On the other hand, the configuration in $[(\eta^5\text{-}C_5Me_5)ClM(\mu\text{-L})MCl(\eta^5\text{-}C_5Me_5)]^+$ produces a singly occupied L-centered MO with closer-lying unoccupied MOs (d or other π^* MOs of L), which results in lowered g values relative to g(electron) = 2.0023.[31]

The paramagnetic product $[(\eta^5\text{-}C_5Me_5)M(\mu\text{-L})M(\eta^5\text{-}C_5Me_5)]^-$ resulting from the last cyclovoltammetrically observed reduction process could not be studied by EPR because of slow dissociation at the very negative potentials required.

UV/Vis/NIR Spectroelectrochemistry of Paramagnetic Intermediates. The appearance of absorptions in the long-wavelength region of the visible spectrum or even in the near-infrared (NIR) is a typical phenomenon associated with mixed valency.[1−13] These transitions can be approximated as intervalence charge-transfer (IVCT) transitions for a localized formulation $L_nM^k(\mu\text{-L})M^{k+1}L_n$ or as $\pi \rightarrow \pi^*$ transitions of a dimetallic π system in a delozalized description. Numerical approximations as the one by Hush[1−4,32] have been used to relate these transitions (energy, oscillator strength) with electronic coupling energies.

Using spectroelectrochemical techniques with an optically transparent thin-layer electrochemical cell,[19] we have studied the complexes by absorption spectroscopy in the visible and NIR region. The starting materials are characterized by ^{1}LMCT (Rh, Ir) and ^{3}LMCT (Ir) transitions in the visible (LMCT: ligand-to-metal charge transfer).

The one-electron-reduced forms of the bxip complexes are not sufficiently persistent on the time scale needed for conventional spectroelectrochemical measurements (>1 min). The electrolysis at the first reduction peak leads directly to the two-electron reduction product because of a disproportionation reaction (see cyclic voltammetry chapter above), and consequently, the second reduction peak (B in Figure 1) is suppressed. The three-electron reduction product $[(\eta^5\text{-}C_5Me_5)M(\mu\text{-bxip})MCl(\eta^5\text{-}C_5Me_5)]^+$ can be generated when the potential is scanned slowly at the beginning of the overlapping peaks C and D. The one-electron-reduced cations $[(\eta^5\text{-}C_5Me_5)ClM(\mu\text{-bpip})MCl(\eta^5\text{-}C_5Me_5)]^+$ exhibit only intraligand (IL) and ligand-to-metal charge transfer (LMCT) transitions in the visible according to their formulation as radical complexes.[31] On the other hand, the chloride-free cations $[(\eta^5\text{-}C_5Me_5)M(\mu\text{-L})M(\eta^5\text{-}C_5Me_5)]^+$ exhibit a series of at least two bands of medium intensity ($\epsilon \approx 2000$ M^{-1} cm^{-1}) in the NIR, viz., in the region between 900 and 1800 nm (Figure 3, Table 3). For comparison, the Creutz−Taube ion absorbs at 1585 nm in DMF solution.[23]

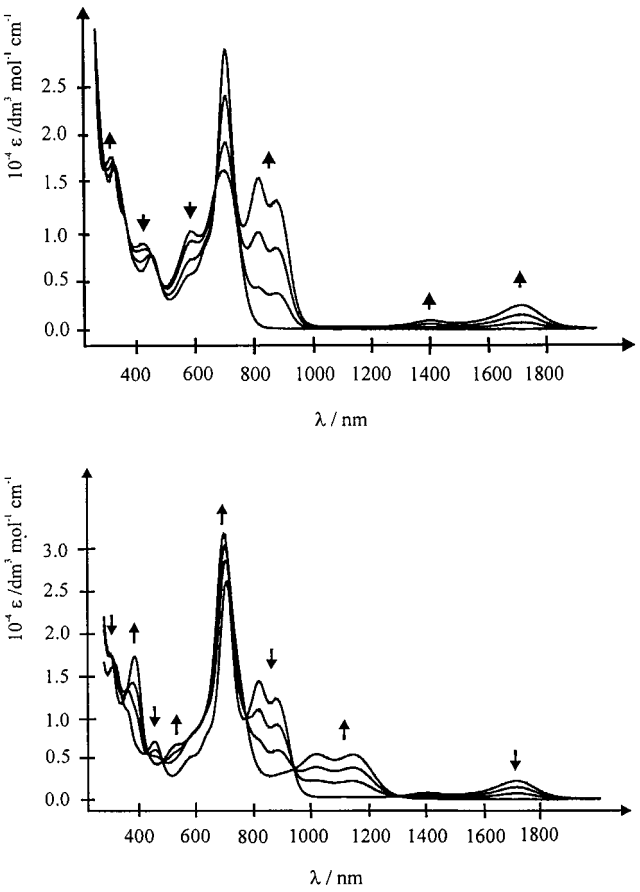

Figure 3. Spectroelectrochemical response for the transitions $[(\eta^5\text{-}C_5Me_5)Rh(\mu\text{-bxip})RhCl(\eta^5\text{-}C_5Me_5)]^+ \rightarrow [(\eta^5\text{-}C_5Me_5)Rh(\mu\text{-bxip})Rh(\eta^5\text{-}C_5Me_5)]^+$ (upper spectrum) and $[(\eta^5\text{-}C_5Me_5)Rh(\mu\text{-bxip})Rh(\eta^5\text{-}C_5Me_5)]^{(+)\rightarrow(0)}$ (lower spectrum) in the UV/vis/NIR region (DMF/0.1 M Bu_4NPF_6).

The separation between individual components of about 1100−1600 cm^{-1} supports their assignment as vibrational components of one allowed electronic transition.[33−36] Chelate complexes of the $(\eta^5\text{-}C_5Me_5)M$ fragments are known to exhibit such phenomena because of their rigidity and relatively small number of rotational and vibrational degrees of freedom.[33−36]

As has been observed previously,[21] the IVCT energy is higher for the iridium species because of the stronger coupling of the 5d metal centers. The difference between bpip and bxip compounds is marginal. The neutral $[(\eta^5\text{-}C_5Me_5)M(\mu\text{-L})M(\eta^5\text{-}C_5Me_5)]$ complexes also exhibit a series of long-wavelength bands in the near-IR albeit at higher energies than the corresponding cations. According to previous findings for mononuclear compounds $(\eta^5\text{-}C_5Me_5)M(\alpha\text{-diimine})$[24−26,33−35] there is extensive charge transfer to the chelate ligand, which allows for possible mixed-valent resonance structures such as $[(\eta^5\text{-}C_5Me_5)M^I(\mu\text{-}L^{\bullet-})M^{II}(\eta^5\text{-}C_5Me_5)]$.

(31) Kaim, W. *Coord. Chem. Rev.* **1987**, *76*, 187.
(32) Hush, N. S. *Coord. Chem. Rev.* **1985**, *64*, 135.
(33) Ladwig, M.; Kaim, W. *J. Organomet. Chem.* **1991**, *419*, 233.
(34) Ladwig, M.; Kaim, W. *J. Organomet. Chem.* **1992**, *439*, 79.
(35) Kaim, W.; Reinhardt, R.; Waldhör, E.; Fiedler, J. *J. Organomet. Chem.* **1996**, *524*, 195.
(36) Kaim, W.; Reinhardt, R.; Sieger, M. *Inorg. Chem.* **1994**, *33*, 4453.

Table 3. Absorption Maxima[a] of Complexes from UV/Vis/NIR Spectroelectrochemistry[b]

μ-L = bpip		μ-L = bxip	
M = Ir	M = Rh	M = Ir	M = Rh
	$[(\eta^5\text{-}C_5Me_5)ClM(\mu\text{-}L)MCl(\eta^5\text{-}C_5Me_5)]^{2+}$		
320 (11.6)	321 (14)	292 (7.0)	310 (13)
380 sh (7.7)	370 (11)		400 (8.6)
504 (10.3)	465 (10)	514 (9.5)	474 (7.3)
610 (2.9)[c]		602[c] (5.4)	
	$[(\eta^5\text{-}C_5Me_5)ClM(\mu\text{-}L)MCl(\eta^5\text{-}C_5Me_5)]^{\bullet+}$		
360 (10.5)	330 (14)	*e*	*e*
387 (10.7)	402 (14)		
480 (11.6)	451 (13)		
533 (8.7)	546 (9)		
636 (7.6)	690 (4)		
860 (0.1)[c]			
	$[(\eta^5\text{-}C_5Me_5)M(\mu\text{-}L)MCl(\eta^5\text{-}C_5Me_5)]^{+}$		
300 (17.2)	321 (21)	297 (19)	328 (17)
382 (16.6)	429 (10)	372 (15)	422 (8.5)
530 (18.2)	578 (12)	534 (16)	588 (10)
625 (11.0)	691 (18)	629 (10)	702 (16)
	$[(\eta^5\text{-}C_5Me_5)M(\mu\text{-}L)M(\eta^5\text{-}C_5Me_5)]^{+}$		
285[d]	311 (21)	340[d]	313(17)
	362 (11)		362 (11)
378	452 (7)	376	456 (7.4)
495 sh		491	
530	578 (7)	527	578 (5.4)
		626	
680	698 (29)	682	706 (28)
	805 (12)		820 (15)
825	877 (9)	825	875 (13)
1070	1142 (0.9)	925	
1225	1396 (1.1)	1234	1406 (0.8)
1415	1708 (3.2)	1405	1717 (2.3)
	$[(\eta^5\text{-}C_5Me_5)M(\mu\text{-}L)M(\eta^5\text{-}C_5Me_5)]$		
344 (14.7)	298 (19)	344 (16)	298 (19)
412 (13.1)	383 (17)	412 (14)	385 (18)
527 (11.8)	523 (7)	528 (13)	522 (6.9)
703 (19.5)	698 (33)	702 (29)	698 (34)
926 (0.9)	886 (6)	928 (2.3)	902 (3.4)
1050 (1.9)	1007 (5)	1008 (3.1)	1016 (5.7)
1205 (1.8)	1136 (5)	1199 (1.9)	1142 (5.7)

[a] Absorption maxima λ_{max} in nm (molar extinction coefficients $\epsilon \times 10^{-3}$ in M^{-1} cm^{-1}). [b] OTTLE cell: CH_3CN/0.1 M Bu_4NPF_6 for L = bpip and DMF/0.1 M Bu_4NPF_6 for L = bxip. [c] ^{3}LMCT. [d] Observed within comproportionation equilibrium. [e] Not observed because of low stability (see text).

Concluding Remarks

One-electron uptake by complexes $[(\eta^5\text{-}C_5Me_5)ClM(\mu\text{-}L)MCl(\eta^5\text{-}C_5Me_5)]^{2+}$ with 2,5-diiminopyrazine bridging ligands L produces $L^{\bullet-}$-containing species after reversible (L = bpip) or partially irreversible processes (L = bxip). Addition of two more electrons yields chloride-free paramagnetic species $[(\eta^5\text{-}C_5Me_5)M(\mu\text{-}L)M(\eta^5\text{-}C_5Me_5)]^{+}$ whose EPR data (*g* anisotropy) and spectroelectrochemical characteristics (near-infrared IVCT absorption) suggest a metal−metal mixed-valent situation involving divalent rhodium[37] or iridium.[30] The comparatively small *g* anisotropy especially for the iridium systems indicates some ($\eta^5\text{-}C_5Me_5$) coligand participation in the SOMO due to partial covalent bonding; similar effects were noted for organometallic $Mo_2^{0,I}$ and $W_2^{0,I}$ compounds.[5,6] In the absence of EPR hyperfine or direct IR vibrational data, the question[7] of valence localization or delocalization cannot be unambiguously answered; the small potential splitting of less than 150 mV between neigboring redox waves is more compatible with a localized description. The oxidation state and d electron configuration assignment to the metals is also not immediately obvious for compounds $[(\eta^5\text{-}C_5Me_5)M(\mu\text{-}L)M(\eta^5\text{-}C_5Me_5)]^{+}$; the ability of $(\eta^5\text{-}C_5Me_5)M$ (M = Rh,Ir) fragments to transfer large amounts of negative charge to bound α-diimine acceptor sites[24−26,33−35] points to a resonance situation

$$[(\eta^5\text{-}C_5Me_5)M^{II}(\mu\text{-}L)M^{I}(\eta^5\text{-}C_5Me_5)]^{+} \rightleftharpoons [(\eta^5\text{-}C_5Me_5)M^{II}(\mu\text{-}L^{\bullet-})M^{II}(\eta^5\text{-}C_5Me_5)]^{+} \rightleftharpoons [(\eta^5\text{-}C_5Me_5)M^{III}(\mu\text{-}L^{2-})M^{II}(\eta^5\text{-}C_5Me_5)]^{+} \quad (1)$$

that was similarly observed for diruthenium(II,III) complexes.[14]

A π acceptor ligand mediated d^7/d^8 (M^{II}/M^{I}) mixed-valent configuration would be compatible with the established electronic structure of the $(\eta^5\text{-}C_5Me_5)M$(α-diimine) moiety.[24] In contrast, square planar diplatinum(III,II) complexes with their different d orbital ordering are less favored for π ligand-mediated metal−metal interaction.[18]

Acknowledgment. Support for this work from Deutsche Forschungsgemeinschaft, Volkswagenstiftung, Fonds der Chemischen Industrie and the Czech Ministry of Education (Grant OC D15.10) is gratefully acknowledged. We also thank Degussa-Hüls AG for providing us with precious metal precursor compounds.

Supporting Information Available: Figures of cyclic voltammograms and EPR spectra. This material is available free of charge via the Internet at http://pubs.acs.org.

IC991110D

(37) (a) DeWit, D. G. *Coord. Chem. Rev.* **1996**, *147*, 209. (b) Pandey, K. K. *Coord. Chem. Rev.* **1992**, *121*, 1.